Inorganic Chemistry

Article

pubs.acs.org/IC

Luminescent Coordination Glass: Remarkable Morphological Strategy for Assembled Eu(III) Complexes

Yuichi Hirai,[†] Takayuki Nakanishi,[†] Yuichi Kitagawa,[†] Koji Fushimi,[†] Tomohiro Seki,[†] Hajime Ito,[†] Hiroyuki Fueno,[‡] Kazuyoshi Tanaka,[‡] Toshifumi Satoh,[†] and Yasuchika Hasegawa*[,†]

[†]Faculty of Engineering, Hokkaido University, N13 W8, Kita-ku, Sapporo, Hokkaido 060-8628, Japan

[‡]Graduate School of Engineering, Kyoto University, Nishikyo-ku, Kyoto 615-8510, Japan

Supporting Information

ABSTRACT: Syntheses of novel luminescent Eu(III) coordination glasses **1** ($[Eu(hfa)_3(o\text{-dpeb})]_2$), **2** ($[Eu(hfa)_3(m\text{-dpeb})]_3$), and **3** ($[Eu(hfa)_3(p\text{-dpeb})]_n$) are reported. They are composed of Eu(III) ions, hexafluoroacetylacetonato (hfa) ligands, and unique bent-angled phosphine oxide (*o*-, *m*-, *p*-dpeb) ligands with ethynyl groups. Their coordination structures and glass formability are dependent on the regiochemistry of substitution in regard to the internal benzene core. Single-crystal X-ray analyses and DFT calculation reveals dinuclear, trinuclear, and polymer structures for Eu(III) coordination glasses **1**, **2**, and **3**, respectively. Those compounds show characteristic glass-transition (T_g = 25−96 °C) and strong luminescence properties (Φ_{Ln} = 72−94%).

INTRODUCTION

Amorphous inorganic and organic compounds have opened up a new field of materials science.[1−4] In particular, small organic molecules that readily form amorphous solids are referred to as "amorphous molecular materials". They have recently attracted attention as a novel class of functional materials with characteristic processability, transparency, isotropic, and homogeneous properties for optical applications.[5,6] π-Conjugated organic molecules with stable amorphous glass structures above room temperature have previously been investigated for use in devices such as organic electroluminescence (EL) and field-effect transistor (FET) devices.[7,8] Shirota and co-workers reported that various types of organic molecules with C_3-symmetric starburst triphenylamines, triarylbenzenes, and tris(oligoarylenyl)boranes form stable amorphous solid and show effective charge transfer abilities.[9,10] Tian demonstrated the remarkable glass-forming ability of small molecules with electron-accepting 2-pyran-4-ylidenemalononitrile.[11] Balcerzak recently succeeded in synthesizing thermostable molecular glasses composed of thiophene rings, diimide, and imine units (T_g > 300 °C).[12]

In this study, we present a luminescent glass based on lanthanide coordination complexes as a new class of amorphous molecular material with 4f−4f emissions. Lanthanide complexes are generally composed of lanthanide ions and π-conjugated organic ligands.[13,14] Their 4f−4f emissions are based on the parity-forbidden transitions with small offset, which lead to characteristic emission with high color purity and long emission lifetimes.[15−17] Excitation at the π−π^* transition of organic ligands also leads to effective photosensitized luminescence of lanthanide complexes.[18,19] In particular, lanthanide complexes with β-diketonate ligands are well known for their strong luminescence properties.[20−24]

Control of the molecular morphology, which dominates the molecular motion and packing structure, is thus required to construct amorphous lanthanide complexes. Bazan and co-workers developed an amorphous Eu(III) complex by introducing the hexyloxy groups in order to prevent their crystallization.[25] Generally, long alkyl chains in the Eu(III) complexes improve their solubility and amorphous formability. In contrast, the long alkyl chains and organic matrices including high-vibrational frequency C−H bonds might have an effect on the nonradiative relaxation of Eu(III) complexes.[26,27] In order to prepare an ideal amorphous lanthanide complex with strong luminescence properties, we considered the importance of specific molecular structures without long alkyl chains. The specific ligand structure for lanthanide complexes may provide formation of ideal amorphous and strong luminescence properties. We previously reported crystalline Eu(III) complexes linked with 1,2-, 1,3-, and 1,4-bis(diphenylphosphoryl)-benzene ligands.[28,29] Introduction of ethynyl groups into these bridging ligands would be expected to suppress tight-binding interactions and crystallization in assembled Eu(III) complexes, while Eu(III) complexes with ethynyl groups show characteristic two-photon absorption properties.[30,31]

In this study, the novel lanthanide complexes with amorphous and strong luminescent properties are demon-

Received: January 21, 2015
Published: April 15, 2015

DOI: 10.1021/acs.inorgchem.5b00145
Inorg. Chem. 2015, 54, 4364−4370

strated. The lanthanide complexes are composed of Eu(III) ions, low-vibrational frequency hexafluoroacetylacetonato anions (hfa), and characteristic *o*-, *m*-, *p*-dpeb: 1,2-, 1,3-, and 1,4-bis(diphenylphosphorylethynyl)benzene) ligands (Figure 1). Ethynyl groups in the dpeb ligands play an important role

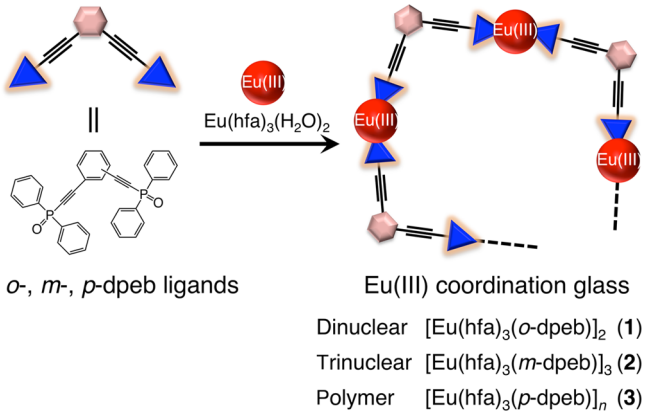

Figure 1. Conceptual diagram of formation of Eu(III) coordination glass.

to prevent $\pi-\pi$ and CH$-\pi$ interactions, although phenylene-linked joint ligands promote tight-packing structures between the molecules.[29,32] The morphological properties were characterized using X-ray single-crystal structural analyses, scanning probe microscope (SPM), and differential scanning calorimetry (DSC) measurements. The luminescent properties were estimated from the radiative and nonradiative constants based on the emission quantum yields and emission lifetimes. The amorphous lanthanide complexes with transparent glass states, referred to as lanthanide coordination glass, exhibit remarkable luminescence properties. The lanthanide coordination glasses are expected to open up a new field of material science using strong luminescent thin films such as organic EL devices.

EXPERIMENTAL SECTION

General Methods. All chemicals were reagent grade and used without further purification. Infrared spectra were recorded on a JASCO FT/IR-420 spectrometer. ESI-MS spectra were measured using a JEOL JMS-T100LP and a Thermo Scientific Exactive. FAB-MS spectra were recorded on a JEOL JMS-700TZ. Elemental analyses were performed on a J-Science Lab JM 10 Micro Corder and an Exeter Analytical CE440. ^{1}H NMR (400 MHz) spectra were recorded on a JEOL ECS400. ^{13}C NMR (100 MHz) and ^{31}P NMR (162 MHz) spectra were recorded on a JEOL ECX400. Chemical shifts were reported in δ ppm, referenced to an internal tetramethylsilane standard for ^{1}H NMR and internal 85% H_3PO_4 standard for ^{31}P NMR. Differential thermal analysis was performed on a Shimadzu DSC-60 Plus under an argon atmosphere at a heating/cooling rate of 5 °C min^{-1}. Surface observation was conducted by a Shimadzu SPM-9700.

1,2-Bis(diphenylphosphorylethynyl)benzene (o-dpeb). Trimethylsilylacetylene (3.4 g, 35 mmol) was added in one portion to a degassed solution of 1,2-diiodobenzene (**A**, 2.0 mL, 15 mmol), $Pd(PPh_3)_2Cl_2$ (0.5 g, 0.7 mmol), and CuI (0.5 g, 2.5 mmol) in diisopropylamine (100 mL) at room temperature. The mixture was refluxed under argon for 4 h, ammonium salt was removed by filtration, and the solvent was evaporated in vacuo. The residue was purified by column chromatography on SiO_2 using hexanes as an eluent to afford 1,2-bis(trimethylsilylethynyl)benzene.[33] The resulting 1,2-bis-(trimethylsilylethynyl)benzene (3.8 g, 14 mmol) was dissolved in methanol (50 mL), and 1 M K_2CO_3 aqueous solution (35 mL, 35 mmol) was added. The mixture was stirred for 3 h. The product was extracted with diethyl ether, washed with brine three times, and dried over anhydrous $MgSO_4$. The solvent was evaporated to afford 1,2-diethynylbenzene (**B**).[34] Compound **B** was dissolved in dry diethyl ether (60 mL), and a solution of *n*-BuLi (19 mL, 31 mmol) was added dropwise at −80 °C in ca. 15 min. The mixture was allowed to stir for 3 h at −10 °C, after which PPh_2Cl (5.8 mL, 31 mmol) was added dropwise at −80 °C. The mixture was gradually brought to room temperature and stirred for 14 h. The product was extracted with dichloromethane, washed with brine three times, and dried over anhydrous $MgSO_4$. The solvent was evaporated, and the obtained pale yellow solid was placed with dichloromethane (50 mL) in a flask. The solution was cooled to 0 °C, and then 30% H_2O_2 aqueous solution (6.0 mL) was added to it. The reaction mixture was stirred for 2 h. The product was extracted with dichloromethane; the extracts were purified by column chromatography on SiO_2 using ethyl acetate and hexanes as mixed eluent (ethyl acetate: hexane = 2:1) to afford *o*-dpeb; yield 2.3 g (29%). ^{1}H NMR (400 MHz, $CDCl_3$, 25 °C): δ 7.79−7.86 (m, 8H, −CH), δ 7.64−7.67 (m, 2H, −CH), δ 7.43−7.49 (m, 6H, −CH), δ 7.35−7.41 (m, 8H, −CH) ppm. ^{13}C NMR (100 MHz, $CDCl_3$, 25 °C): δ 133.8, 133.2, 132.4, 131.9, 131.0, 130.9, 130.6, 128.9, 128.8, 123.2, 102.3, 102.0, 88.6, 86.9 ppm. ^{31}P NMR (162 MHz, $CDCl_3$, 25 °C): δ 9.17 (s, 2P) ppm. ESI-Mass (m/z): $[M + H]^+$ calcd for $C_{34}H_{25}O_2P_2$, 527.1; found, 527.1. Anal. Calcd for $C_{34}H_{24}O_2P_2$: C, 77.56; H, 4.59. Found: C, 77.99; H, 4.58.

1,3-Bis(diphenylphosphorylethynyl)benzene (m-dpeb). The 1,3-diethynylbenzene (**C**, 1.8 g, 14 mmol) was dissolved in dry diethyl ether (60 mL), and the mixture was degassed by Ar bubbling for 20 min. A solution of *n*-BuLi (19 mL, 31 mmol) was added dropwise to the solution at −80 °C. The addition was completed in ca. 15 min, during which time a yellow precipitate was formed. The mixture was allowed to stir for 3 h at −10 °C, after which PPh_2Cl (5.8 mL, 31 mmol) was added dropwise at −80 °C. The mixture was gradually brought to room temperature and stirred for 14 h. The product was extracted with dichloromethane; the extracts were washed with brine three times and dried over anhydrous $MgSO_4$. The solvent was evaporated, and the obtained pale yellow solid was placed with dichloromethane (50 mL) in a flask. The solution was cooled to 0 °C, and then 30% H_2O_2 aqueous solution (6.0 mL) was added to it. The reaction mixture was stirred for 2 h. The product was extracted with dichloromethane; the extracts were purified by column chromatography on SiO_2 using ethyl acetate and hexanes as mixed eluent (ethyl acetate:hexane = 2:1) to afford *m*-dpeb; yield 4.3 g (58%). ^{1}H NMR (400 MHz, $CDCl_3$, 25 °C): δ 7.84−7.95 (m, 8H, −CH), δ 7.82 (s, 1H, −CH), δ 7.67−7.70 (d, 1H, −CH), δ 7.64−7.66 (d, 1H, −CH), δ 7.47−7.62 (m, 12H, −CH), δ 7.38−7.46 (t, 1H, −CH) ppm. ^{13}C NMR (100 MHz, $CDCl_3$, 25 °C): δ 136.3, 134.4, 133.3, 132.5, 132.0, 131.1, 131.0, 129.2, 128.9, 128.8, 120.9, 103.3, 103.0, 85.4, 83.7 ppm. ^{31}P NMR (162 MHz, $CDCl_3$, 25 °C): δ 9.01 (s, 2P) ppm. ESI-Mass (m/z): $[M + H]^+$ calcd for $C_{34}H_{25}O_2P_2$, 527.1; found, 527.1. Anal. Calcd for $C_{34}H_{24}O_2P_2$: C, 77.56; H, 4.59. Found: C, 77.70; H, 4.64.

1,4-Bis(diphenylphosphorylethynyl)benzene (p-dpeb). 1,4-Bis-(diphenylphosphorylethynyl)benzene (*p*-dpeb) was obtained using the same method for *m*-dpeb, starting from 1,4-diethynylbenzene (**D**); yield 4.8 g (65%). ^{1}H NMR (400 MHz, $CDCl_3$, 25 °C): δ 7.84−7.90 (m, 8H, −CH), δ 7.59 (s, 4H, −CH), δ 7.55−7.56 (d, 4H, −CH), δ 7.47−7.51 (m, 8H, −CH) ppm. ^{13}C NMR (100 MHz, $CDCl_3$, 25 °C): δ 133.2, 132.7, 132.6, 132.0, 131.1, 131.0, 128.9, 122.2, 103.9, 103.6, 86.8, 85.1 ppm. ^{31}P NMR (162 MHz, $CDCl_3$, 25 °C): δ 9.06 (s, 2P) ppm. ESI-Mass (m/z): $[M + H]^+$ calcd for $C_{34}H_{25}O_2P_2$, 527.1; found, 527.1. Anal. Calcd for $C_{34}H_{24}O_2P_2$: C, 77.56; H, 4.59. Found: C, 77.52; H, 4.72.

$[Eu(hfa)_3$(o-dpeb)$]_2$ (1), $[Eu(hfa)_3$(m-dpeb)$]_3$ (2), and $[Eu(hfa)_3$(p-dpeb)$]_n$ (3). Phosphine oxide ligands (*o*-, *m*-, or *p*-dpeb; 0.21 g, 0.40 mmol) and $Eu(hfa)_3(H_2O)_2$ (0.32 g, 0.40 mmol) were dissolved in methanol. The solutions were stirred for 2 h at room temperature. The solvent was evaporated, and the obtained white solid was washed with chloroform and hexanes.

1: Yield 0.27 g (26%). IR (ATR) 1657 (st, C=O), 1132 (st, P=O), 1093−1249 (st, C−O−C and st, C−F) cm^{-1}. FAB-Mass (m/z):

DOI: 10.1021/acs.inorgchem.5b00145
Inorg. Chem. 2015, 54, 4364−4370

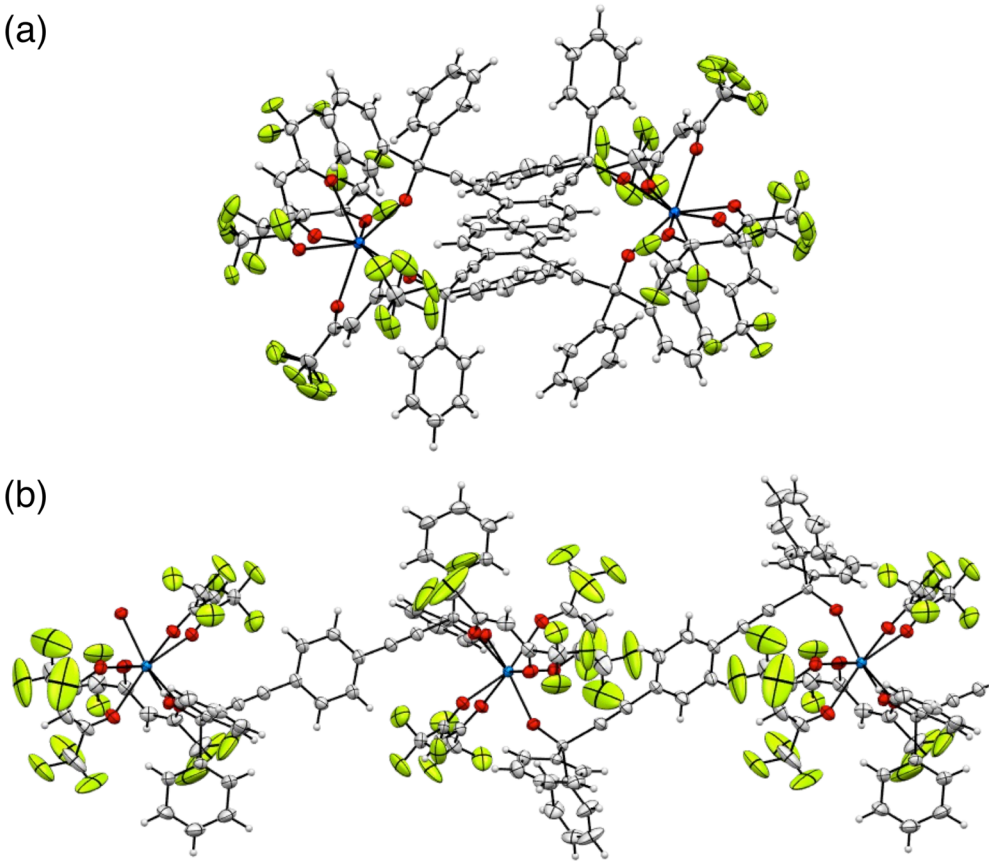

Figure 2. Perspective view of (a) complex **1** and (b) complex **3**, showing 50% probability displacement ellipsoids.

$[M - hfa]^+$ calcd for $C_{93}H_{53}Eu_2F_{30}O_{14}P_4$, 2392.2; found, 2392.0. Anal. Calcd for: C, 45.29; H, 2.09. Found: C, 45.05; H, 2.21.

2: Yield 0.34 g (22%). IR (ATR) 1657 (st, C═O), 1142 (st, P═O), 1093−1258 (st, C−O−C and st, C−F) cm^{-1}. FAB-Mass (m/z): $[M - hfa]^+$ calcd for $C_{142}H_{80}Eu_3F_{48}O_{22}P_6$, 3691.8; found, 3691.8. Anal. Calcd for: C, 45.29; H, 2.09. Found: C, 45.34; H, 1.68.

3: Yield 0.39 g (75%; for monomer). IR (ATR) 1657 (st, C═O), 1141 (st, P═O), 1093−1249 (st, C−O−C and st, C−F) cm^{-1}. FAB-Mass (m/z): $[M - hfa]^+$ calcd for $C_{44}H_{26}EuF_{12}O_6P_2$, 1092.6; found, 1092.7. Anal. Calcd for: C, 45.29; H, 2.09. Found: C, 44.98; H, 2.18.

Optical Measurements. UV−vis absorption spectra were recorded on a JASCO V-670 spectrometer. Emission and excitation spectra were recorded on a HORIBA Fluorolog-3 spectrofluorometer and corrected for the response of the detector system. Emission lifetimes (τ_{obs}) were measured using the third harmonics (355 nm) of a Q-switched Nd:YAG laser (Spectra Physiscs, INDI-50, fwhm = 5 ns, λ = 1064 nm) and a photomultiplier (Hamamatsu photonics, R5108, response time ≤ 1.1 ns). The Nd:YAG laser response was monitored with a digital oscilloscope (Sony Tektronix, TDS3052, 500 MHz) synchronized to the single-pulse excitation. Emission lifetimes were determined from the slope of logarithmic plots of the decay profiles. The emission quantum yields excited at 380 nm (Φ_{tot}) were estimated using a JASCO F-6300-H spectrometer attached with JASCO ILF-53 integrating sphere unit (φ = 100 nm). The wavelength dependence of the detector response and the beam intensity of the Xe light source for each spectrum were calibrated using a standard light source.

Single-Crystal X-ray Structure Determinations. The X-ray crystal structures and crystallographic data for complexes **1** and **3**, recrystallized from methanol, are shown in Figure 2 and Table 1. Colorless single crystals of the complexes were mounted on a MiTeGen micromesh using paraffin oil. All measurements were made on a Rigaku RAXIS RAPID imaging plate area detector with graphite monochromated MoKα radiation. Correction for decay and Lorentz-polarization effects were made using empirical absorption correction,

Table 1. Crystallographic Data

	complex **1**	complex **3**
chemical formula	$C_{98}H_{54}Eu_2F_{36}O_{16}P_4$	$C_{49}H_{27}EuF_{18}O_8P_2$
fw	2599.25	1299.63
cryst syst	monoclinic	monoclinic
space group	$P2_1/n$ (no. 14)	$P2_1/c$ (no. 14)
a (Å)	12.5432(9)	23.1941(10)
b (Å)	30.3644(15)	13.4114(5)
c (Å)	12.9212(9)	16.7226(6)
α (deg)	90.000	90.000
β (deg)	90.378(6)	91.6148(10)
γ (deg)	90.000	90.000
vol. (Å^3)	4921.1(5)	5199.8(4)
Z	2	4
d_{calcd} (g cm^{-3})	1.754	1.660
temp (°C)	23.0	−150
μ (Mo Kα) (cm^{-1})	14.590	13.809
max 2θ (deg)	55.0	55.00
no. of reflns collected	48 310	49 124
no. of independent reflns	11 257	11 871
R_1	0.0439	0.0420
wR_2	0.0728	0.0998

$^a R_1 = \Sigma||F_0| - |F_c||/\Sigma|F_0|$. $^b wR_2 = [\Sigma w(F_0^2 - F_c^2)^2/\Sigma w(F_0^2)^2]^{1/2}$.

solved by direct methods and expanded using Fourier techniques. Non-hydrogen atoms were refined anisotropically. Hydrogen atoms were refined using the riding model. The final cycle of full-matrix least-squares refinement was based on observed reflections and variable parameters. All calculations were performed using the crystal structure crystallographic software package. The CIF data was confirmed by the checkCIF/PLATON service. CCDC-1037529 (for complex **1**) and

DOI: 10.1021/acs.inorgchem.5b00145
Inorg. Chem. 2015, 54, 4364−4370

CCDC 1037531 (for complex **3**) contain the supplementary crystallographic data for this paper. These data can be obtained free of charge from The Cambridge Crystallographic Data Centre via www.ccdc.cam.ac.uk/data_request/cif.

DFT Calculations. Due to the lack of structural data of Eu(III) complex **2**, Figure 3, the DFT calculation was carried out at the B3LYP level with the basis sets SDD for Eu and 6-31G** for other atoms using the Gaussian 09 program package.[35−38] The ultrafine grid was used for numerical integrations. A trimer structure was plausibly assumed for this complex.

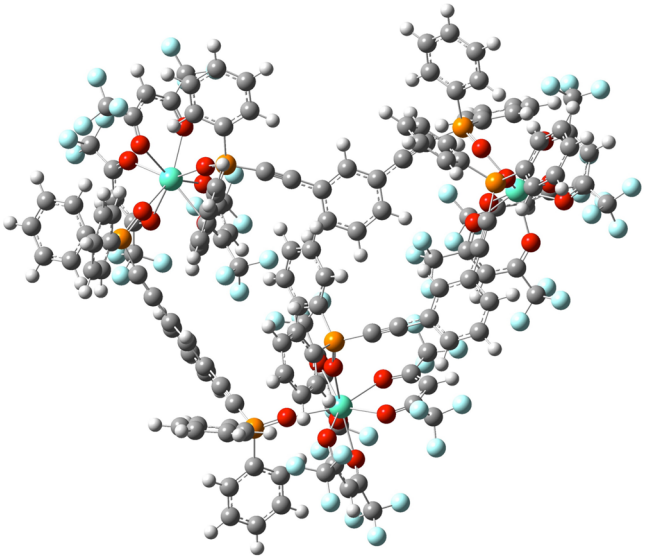

Figure 3. DFT-calculated structure of complex **2**.

RESULTS AND DISCUSSION

$[Eu(hfa)_3(o\text{-dpeb})]_2$ (**1**), $[Eu(hfa)_3(m\text{-dpeb})]_3$ (**2**), and $[Eu(hfa)_3(p\text{-dpeb})]_n$ (**3**) were synthesized by complexation of phosphane oxide ligands (*o*-, *m*-, *p*-dpeb) with $Eu(hfa)_3(H_2O)_2$ in methanol for 2 h (Scheme 1). The single crystals of Eu(III) complexes **1** and **3** are obtained by recrystallization from methanol solution. On the other hand, they readily form amorphous glasses when the melt samples are rapidly cooled.[6] The structures of complexes **1** and **3** were determined by X-ray single-crystal analyses (Figure 2a and 2b) to be eight-coordinated structures with two phosphine oxide ligands (*o*-dpeb or *p*-dpeb) and three hfa ligands.

Complex **1** forms a dinuclear structure composed of two Eu(III) ions, six hfa, and two *o*-dpeb ligands (Figure 2a). The dinuclear structure is fixed with intra- and intermolecular CH/F interactions with distances of 2.63 and 2.74 Å, respectively (Supporting Information, Figure S1). Complex **3** has a coordination polymer structure with intra- and intermolecular CH/F interactions (2.63 and 2.86 Å, respectively).

The selected distances and angles between the Eu and the O atoms directly reflect the coordination geometry. Generally, the coordination geometry of the lanthanide complex is categorized to be an eight-coordinated square antiprism structure (8-SAP) or a trigonal dodecahedron structure (8-TDH). On the basis of the crystal data, we carried out the calculation of the shape factor *S*[39] in order to estimate the degree of distortion of the coordination structure in the first coordination sphere. The *S* value is given by

$$S = \min \sqrt{\left(\frac{1}{m}\right)\sum_{i=1}^{m}(\delta_i - \theta_i)^2} \quad (1)$$

where m, δ_i, and θ_i are the number of possible edges (m = 18 in this study), the observed dihedral angle between planes along the ith edge, and the dihedral angle for the ideal structure, respectively. For complexes **1** and **3**, the *S* values for 8-SAP (point group D_{4d}, S = 6.90°and 5.17°) are smaller than those for 8-TDH (point group D_{2d}, S = 11.1° and 13.5°), suggesting that the 8-SAP structure is less distorted than the 8-TDH structure. We thus determined that the coordination geometry of complexes **1** and **3** are 8-SAP structure (Supporting Information, Figure S2 and Tables S1 and S2). The FAB-MS spectrum of complex **2** reveals a trinuclear structure, $Eu_3(hfa)_8(m\text{-dpeb})_3^+$ (Figure 4a). The X-ray diffraction image and patterns are similar to those for glass ceramics (Figure 4b and 4c).[40] A circular-shaped structure shown in Figure 3 was obtained after the structure-optimization process.

SPM images of crystal surfaces for complexes **1**, **2**, and **3** are shown in Figure 5. We observed several steps on the crystal surface for complex **1**, indicating the high crystallinity of the dinuclear Eu(III) complex. Complex **2** has a smooth surface based on the amorphous structure. We also found that the Eu(III) coordination polymer complex **3** exhibited fiber-like structures on the crystal surface. DSC measurements were conducted to evaluate the thermophysical properties of the Eu(III) complexes (Figure 6: argon atmosphere, heating/cooling rate = 5 °C min^{-1}). We successfully observed that the thermograms of complexes **1** and **2** show endothermic peaks based on the glass transition of amorphous molecules at 25 and 65 °C, respectively. Two glass-transition points were identified for complex **3** at 46 and 96 °C. The characteristic glass-transition phenomena exhibited by complexes **1**, **2**, and **3** are very similar to those shown by previous amorphous organic molecules. The bent angles of the dpeb ligands (60°, 120°, 180°) have an influence on the molecular morphologies and the glass-transition points. We also consider that these glass-transition phenomena of complexes **1**, **2**, and **3** may be caused by the presence of ethynyl groups in the bent-angled dpeb ligands, although Eu(III) coordination polymers composed of phenylene-linked ligands with tight-packing structures have no glass-transition points.[28,29] The packing structures between the Eu(III) coordination parts may be related to their glass-forming ability.

Eu(III) complexes **1** and **3**, recrystallized from methanol solution, are slightly dissolved in organic solvents. The emission spectra for complexes **1**, **2**, and **3** in the solid state are shown in Figure 7a. Emission bands were observed at around 578, 591, 613, 650, and 698 nm and are attributed to the f−f transitions of Eu(III) ($^5D_0-{}^7F_J$: J = 0, 1, 2, 3, and 4, respectively). The stark splitting energy of $^5D_0-{}^7F_2$ is generally dependent on the coordination geometry.[28,41] The spectral shapes including the stark splittings of complexes **1**, **2**, and **3** might be related to their coordination geometry (Supporting Information, Figure S4). Their time-resolved emission profiles of complexes **1** and **3** reveal single-exponential decays with millisecond scale lifetimes. The emission lifetimes observed from the $^5D_0$ excited level (τ_{obs}) were determined from the slope of the logarithmic decay profiles (Figure 7b). The emission lifetimes for complexes **1**, **2**, and **3** were determined to be 1.03 ± 0.007, 1.00 ± 0.002, and 0.93 ± 0.012 ms, respectively. The 4f−4f emission quantum yields (Φ_{Ln}) and the radiative (k_r) and nonradiative (k_{nr})

DOI: 10.1021/acs.inorgchem.5b00145
Inorg. Chem. 2015, 54, 4364−4370

Scheme 1. Synthetic Schemes of Phosphine Oxide Ligands and Eu(III) Complexes[a]

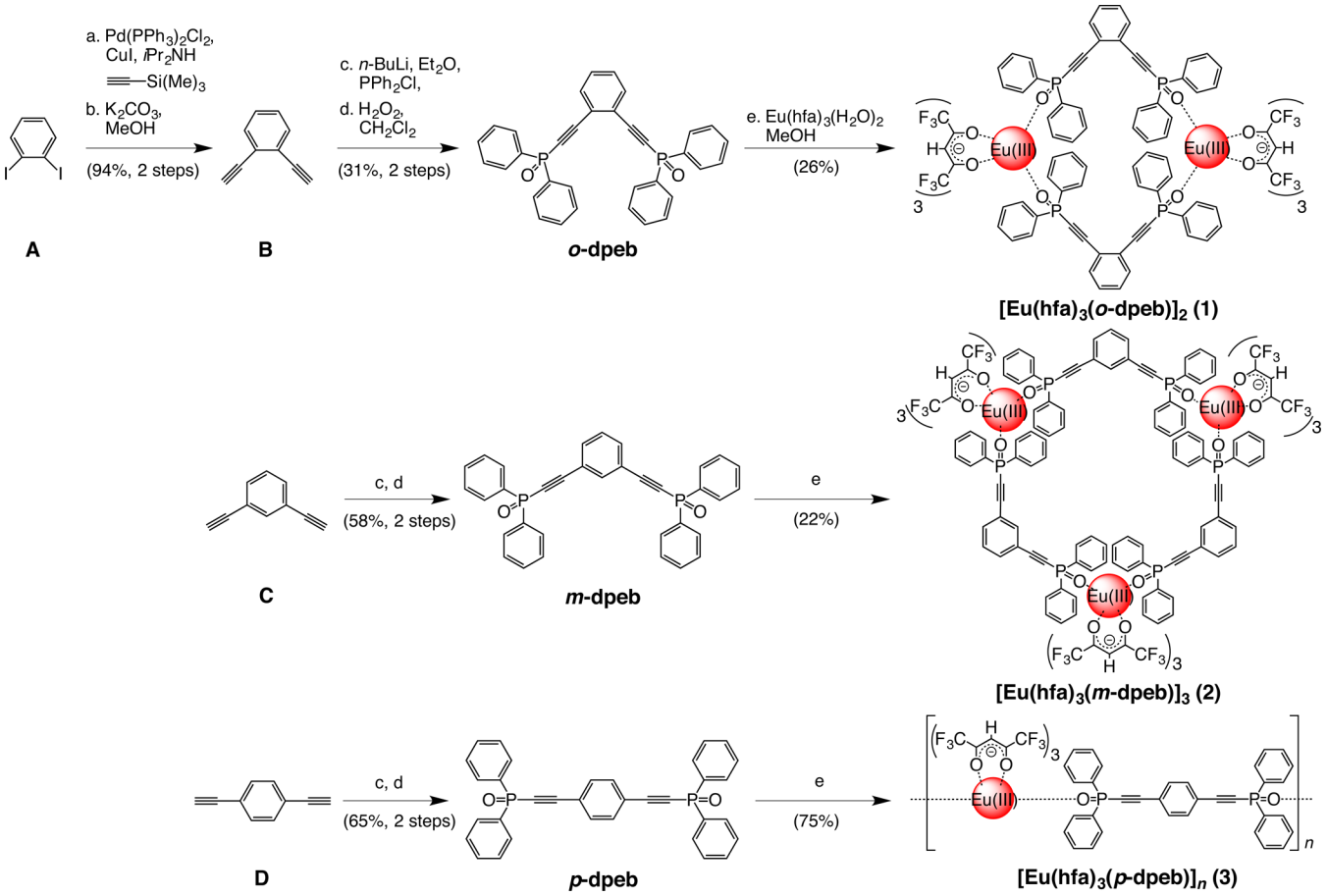

[a]Reagents and conditions: (a) $Pd(PPh_3)_2Cl_2$, CuI, Et_3N, 25 °C then trimethylsilylacetylene, 60°C, reflux; (b) 1 M K_2CO_3, MeOH, 25 °C; (c) *n*-BuLi, Et_2O, −78 °C; then PPh_2Cl, −78 °C; (d) H_2O_2, CH_2Cl_2, 0 °C; (e) $Eu(hfa)_3(H_2O)_2$, MeOH, 25 °C.

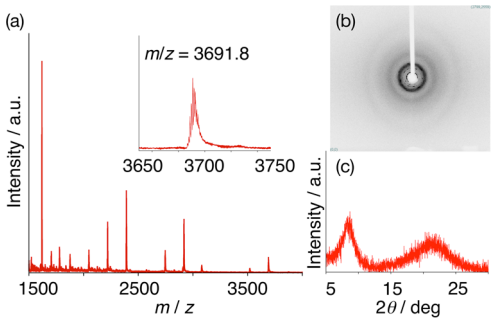

Figure 4. (a) FAB-MS spectrum, (b) X-ray diffraction image, and (c) X-ray diffraction patterns of complex **2**.

constants were estimated (Table 2) using following equations[42,43]

$$\Phi_{ln} = \frac{k_r}{k_r + k_{nr}} = \frac{\tau_{obs}}{\tau_{rad}} \quad (2)$$

$$\frac{1}{\tau_{rad}} = A_{MD,0} n^3 \left(\frac{I_{tot}}{I_{MD}}\right) \quad (3)$$

$$k_r = \frac{1}{\tau_{rad}} \quad (4)$$

$$k_{nr} = \frac{1}{\tau_{obs}} - \frac{1}{\tau_{rad}} \quad (5)$$

where $A_{MD,0}$ is the spontaneous emission probability for the $^5D_0-^7F_1$ transition in vacuo (14.65 s^{-1}), *n* is the refractive index of the medium (an average index of refraction equal to 1.5 was employed[44]), and (I_{tot}/I_{MD}) is the ratio of the total area of the corrected Eu(III) emission spectrum to the area of the $^5D_0-^7F_1$ band. Complex **1** shows a large emission quantum yield (94%), which is based on the large k_r and small k_{nr}. The large k_r for complexes **1** and **3** (9.1×10^2 and 9.2×10^2 s^{-1}) may be due to enhancement of the electric dipole transition probability based on their asymmetric coordination geometries, compared with small k_r for complex **2** (7.2×10^2 s^{-1}). The characteristically small k_{nr} for complex **1** with 60°-angled *o*-dpeb ligands may be induced by the multiple intramolecular CH/F interactions in the dinuclear structures (Figure 2a). The notable amorphous form of luminescent complex **2** with 120°-angled *m*-dpeb ligands is shown in Figure 7c. The amorphous complexes **1**, **2**, and **3** with bent-angled dpeb ligands would be useful for new application such as strong luminescent lanthanide glass.

CONCLUSION

In summary, we successfully controlled the morphological properties of novel luminescent Eu(III) coordination glasses by introducing unique bent-angled phosphine oxide ligands with ethynyl groups. Their coordination structures and glass

DOI: 10.1021/acs.inorgchem.5b00145
Inorg. Chem. 2015, 54, 4364−4370

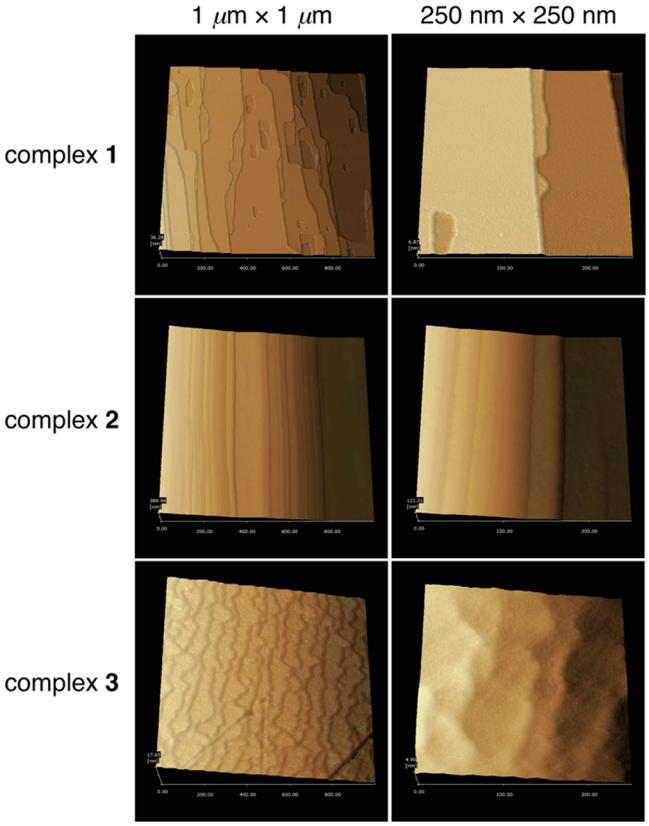

Figure 5. SPM images, 1 μm × 1 μm and 250 nm × 250 nm, of complexes **1**, **2**, and **3**.

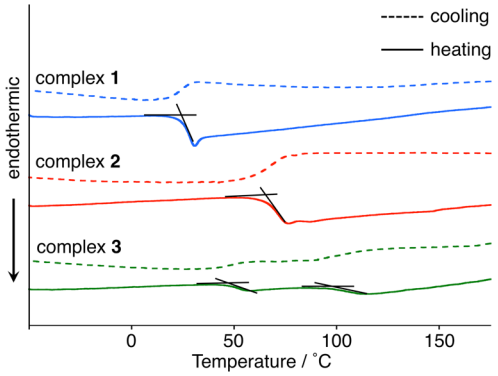

Figure 6. DSC profiles for complexes **1**, **2**, and **3** (dashed line, cooling process; solid line, heating process).

formability are dependent on the regiochemistry of substitution in regard to the internal benzene core. These compounds show characteristic amorphous phase and relatively strong emission. When normal Eu(III) complexes with β-diketonate ligands (absorption coefficient > 30 000 M^{-1} cm^{-1}) are embedded in polymer thin films (thickness = 0.1 μm, dopant concentration = 1 wt %), the absorbance of the films is estimated to be approximately 0.003. On the other hand, absorbance of thin films prepared from Eu(III) coordination glasses may be estimated to be 0.3. These simple estimations for absorbance indicate that Eu(III) coordination glass thin film would be much brighter than those of polymer thin films including normal Eu(III) complexes. We are presently evaluating the electron- or hole-transporting properties of these complexes in the glass state. Lanthanide complexes with glass-transition and

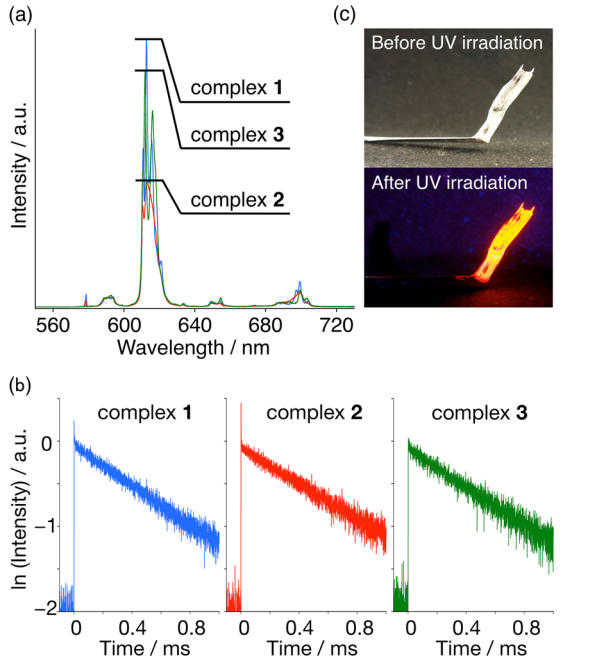

Figure 7. (a) Emission spectra excited at 465 nm, and (b) decay profiles of complexes **1**, **2**, and **3**. (c) Photographs of complex **2** before and after UV irradiation.

Table 2. Photophysical and Thermal Properties of Eu(III) Complexes 1, 2, and 3 in the Solid State

	photophysical properties					
	τ_{obs} (ms)^a	τ_{rad} (ms)^b	Φ_{Ln} (%)^b	k_r (s^{-1})^b	k_{nr} (s^{-1})^b	Φ_{tot} (%)^c
complex **1**	1.0	1.1	94	9.1 × 10^2	6.1 × 10	52
complex **2**	1.0	1.4	72	7.2 × 10^2	2.8 × 10^2	44
complex **3**	0.93	1.1	86	9.2 × 10^2	1.5 × 10^2	54

^{a}Emission lifetime (τ_{obs}) of the Eu(III) complexes were measured by excitation at 355 nm (Nd:YAG 3ω). ^{b}From calculation using eqs 2−5. ^{c}Total emission quantum yield (excited at 380 nm).

strong-luminescence properties, which can be processed at ambient temperatures, are expected to open up a frontier field of coordination chemistry, materials science, and molecular engineering.

■ ASSOCIATED CONTENT

Supporting Information

Crystal structures of **1** and **3**; coordination environments around Eu(III) ion for calculation of S (D_{4d}) and S (D_{2d}) values; observed dihedral angles (δ_i), dihedral angles of idealized square antiprism (θ_i), and measure shape criteria, S (D_{4d}), for complexes **1** and **3**; observed dihedral angles (δ_i), dihedral angles of idealized trigonal dodecahedron (θ_i), and measure shape criteria, S (D_{2d}), for complexes **1** and **3**; absorption and excitation spectra for complexes **1**−**3**; emission spectra of the $^5D_0$−$^7F_2$ band for complexes **1**−**3**. This material is available free of charge via the Internet at http://pubs.acs.org.

■ AUTHOR INFORMATION

Corresponding Author

*Tel./Fax: +81 11 706 7114. E-mail: hasegaway@eng.hokudai.ac.jp.

DOI: 10.1021/acs.inorgchem.5b00145
Inorg. Chem. 2015, 54, 4364−4370

Notes

The authors declare no competing financial interest.

■ ACKNOWLEDGMENTS

This work was financially supported by Grants-in-Aid for Scientific Research on Innovative Areas of "New Polymeric Materials Based on Element-Blocks (No. 2401)" (24102012) of Ministry of Education, Culture, Sports, Science and Technology (MEXT) of Japan. We also appreciate for Shimadzu Corporation and Frontier Chemistry Center Akira Suzuki "Laboratories for Future Creation" Project.

■ REFERENCES

(1) Wang, S. J.; Oldham, W. J.; Hudack, R. A.; Bazan, G. C. *J. Am. Chem. Soc.* **2000**, *122*, 5695−5709.
(2) Reece, S. Y.; Hamel, J. A.; Sung, K.; Jarvi, T. D.; Esswein, A. J.; Pijpers, J. J. H.; Nocera, D. G. *Science* **2011**, *334*, 645−648.
(3) Smith, R. D. L.; Prevot, M. S.; Fagan, R. D.; Zhang, Z. P.; Sedach, P. A.; Siu, M. K. J.; Trudel, S.; Berlinguette, C. P. *Science* **2013**, *340*, 60−63.
(4) Deringer, V. L.; Zhang, W.; Lumeij, M.; Maintz, S.; Wuttig, M.; Mazzarello, R.; Dronskowski, R. *Angew. Chem., Int. Ed.* **2014**, *53*, 10817−10820.
(5) Shirota, Y. *J. Mater. Chem.* **2000**, *10*, 1−25.
(6) Shirota, Y. *J. Mater. Chem.* **2005**, *15*, 75−93.
(7) Mishra, A.; Bäuerle, P. *Angew. Chem., Int. Ed.* **2012**, *51*, 2020−2067.
(8) Costa, J. C. S.; Santos, L. *J. Phys. Chem. C* **2013**, *117*, 10919−10928.
(9) Nakano, H.; Tanino, T.; Takahashi, T.; Ando, H.; Shirota, Y. *J. Mater. Chem.* **2008**, *18*, 242−246.
(10) Nakano, H.; Seki, S.; Kageyama, H. *Phys. Chem. Chem. Phys.* **2010**, *12*, 7772−7774.
(11) Li, Z.; Dong, Q.; Li, Y.; Xu, B.; Deng, M.; Pei, J.; Zhang, J.; Chen, F.; Wen, S.; Gao, Y.; Tian, W. *J. Mater. Chem.* **2011**, *21*, 2159−2168.
(12) Grucela-Zajac, M.; Bijak, K.; Kula, S.; Filapek, M.; Wiacek, M.; Janeczek, H.; Skorka, L.; Gasiorowski, J.; Hingerl, K.; Sariciftci, N. S.; Nosidlak, N.; Lewinska, G.; Sanetra, J.; Schab-Balcerzak, E. *J. Phys. Chem. C* **2014**, *118*, 13070−13086.
(13) Bunzli, J. C. G. *Chem. Rev.* **2010**, *110*, 2729−2755.
(14) Eliseeva, S. V.; Bunzli, J. C. G. *Chem. Soc. Rev.* **2010**, *39*, 189−227.
(15) Nockemann, P.; Beurer, E.; Driesen, K.; Van Deun, R.; Van Hecke, K.; Van Meervelt, L.; Binnemans, K. *Chem. Commun.* **2005**, 4354−4356.
(16) Petoud, S.; Muller, G.; Moore, E. G.; Xu, J. D.; Sokolnicki, J.; Riehl, J. P.; Le, U. N.; Cohen, S. M.; Raymond, K. N. *J. Am. Chem. Soc.* **2007**, *129*, 77−83.
(17) Butler, S. J.; Parker, D. *Chem. Soc. Rev.* **2013**, *42*, 1652−1666.
(18) Bassett, A. P.; Magennis, S. W.; Glover, P. B.; Lewis, D. J.; Spencer, N.; Parsons, S.; Williams, R. M.; De Cola, L.; Pikramenou, Z. *J. Am. Chem. Soc.* **2004**, *126*, 9413−9424.
(19) Armelao, L.; Quici, S.; Barigelletti, F.; Accorsi, G.; Bottaro, G.; Cavazzini, M.; Tondello, E. *Coord. Chem. Rev.* **2010**, *254*, 487−505.
(20) Brito, H. F.; Malta, O.M. L.; Felinto, M. C. F. C.; Teotonio, E. E. S. *Chemistry of Metal Enolates*; 2009; Chapter 3, p 131.
(21) Lima, N. B. D.; Gonçalves, S. M. C.; Junior, S. A.; Simas, A. M. *Sci. Rep.* **2013**, *3*, 1−8.
(22) Borisov, S. M.; Wolfbeis, O. S. *Anal. Chem.* **2006**, *78*, 5094−5101.
(23) Khalil, G. E.; Lau, K.; Phelan, G. D.; Carlson, B.; Gouterman, M.; Callis, J. B.; Dalton, L. R. *Rev. Sci. Instrum.* **2004**, *75*, 192−206.
(24) Eliseeva, S. V.; Pleshkov, D. N.; Lyssenko, K. A.; Lepnev, L. S.; Bunzli, J. C. G.; Kuzminat, N. P. *Inorg. Chem.* **2010**, *49*, 9300−9311.
(25) Robinson, M. R.; O'Regan, M. B.; Bazan, G. C. *Chem. Commun.* **2000**, 1645−1646.
(26) Hasegawa, Y.; Murakoshi, K.; Wada, Y.; Yanagida, S.; Kim, J. H.; Nakashima, N.; Yamanaka, T. *Chem. Phys. Lett.* **1996**, *248*, 8−12.
(27) Hasegawa, Y.; Sogabe, K.; Wada, Y.; Kitamura, T.; Nakashima, N.; Yanagida, S. *Chem. Lett.* **1999**, *1*, 35−36.
(28) Nakamura, K.; Hasegawa, Y.; Kawai, H.; Yasuda, N.; Wada, Y.; Yanagida, S. *J. Alloys Compd.* **2006**, *408*, 771−775.
(29) Miyata, K.; Ohba, T.; Kobayashi, A.; Kato, M.; Nakanishi, T.; Fushimi, K.; Hasegawa, Y. *ChemPlusChem* **2012**, *77*, 277−280.
(30) D'Aleo, A.; Picot, A.; Baldeck, P. L.; Andraud, C.; Maury, O. *Inorg. Chem.* **2008**, *47*, 10269−10279.
(31) Soulie, M.; Latzko, F.; Bourrier, E.; Placide, V.; Butler, S. J.; Pal, R.; Walton, J. W.; Baldeck, P. L.; Le Guennic, B.; Andraud, C.; Zwier, J. M.; Lamarque, L.; Parker, D.; Maury, O. *Chem.—Eur. J.* **2014**, *20*, 8636−8646.
(32) Miyata, K.; Konno, Y.; Nakanishi, T.; Kobayashi, A.; Kato, M.; Fushimi, K.; Hasegawa, Y. *Angew. Chem., Int. Ed.* **2013**, *52*, 6413−6416.
(33) Alabugin, I. V.; Kovalenko, S. V. *J. Am. Chem. Soc.* **2002**, *124*, 9052−9053.
(34) Suresh, P.; Srimurugan, S.; Babu, B.; Pati, H. N. *Acta Chim. Slov.* **2008**, *55*, 453−457.
(35) Tirado-Rives, J.; Jorgensen, W. L. *J. Chem. Theory Comput.* **2008**, *4*, 297−306.
(36) Dolg, M.; Wedig, U.; Stoll, H.; Preuss, H. *J. Chem. Phys.* **1987**, *86*, 866−872.
(37) Maron, L.; Eisenstein, O. *J. Phys. Chem. A* **2000**, *104*, 7140−7143.
(38) Frisch, M. J. et al. *Gaussian 09*, Revision D.01; Gaussian, Inc.: Wallingford, CT, 2009.
(39) Xu, J. D.; Radkov, E.; Ziegler, M.; Raymond, K. N. *Inorg. Chem.* **2000**, *39*, 4156−4164.
(40) Ueda, J.; Tanabe, S. *J. Am. Ceram. Soc.* **2010**, *93*, 3084−3087.
(41) Nakamura, K.; Hasegawa, Y.; Wada, Y.; Yanagida, S. *Chem. Phys. Lett.* **2004**, *398*, 500−504.
(42) Werts, M. H. V.; Jukes, R. T. F.; Verhoeven, J. W. *Phys. Chem. Chem. Phys.* **2002**, *4*, 1542−1548.
(43) Aebischer, A.; Gumy, F.; Bunzli, J.-C. G. *Phys. Chem. Chem. Phys.* **2009**, *11*, 1346−1353.
(44) Pavithran, R.; Kumar, N. S. S.; Biju; Reddy, M. L. P.; Junior, S. A.; Freire, R. O. *Inorg. Chem.* **2006**, *45*, 2184−1292.

DOI: 10.1021/acs.inorgchem.5b00145
Inorg. Chem. 2015, 54, 4364−4370